Journal of Modern Optics

ISSN: 0950-0340 (Print) 1362-3044 (Online) Journal homepage: https://www.tandfonline.com/loi/tmop20

Characterization of detectors for the Italian Astronomical Quantum Photometer Project

Sergio Billotta , Massimiliano Belluso , Giovanni Bonanno , Salvatore di Mauro , Maria Cristina Timpanaro , Giovanni Condorelli , P. Giorgio Fallica , Massimo Mazzillo , Delfo Sanfilippo , Giuseppina Valvo , Luigi Cosentino , Paolo Finocchiaro , Alfio Pappalardo , Giampiero Naletto , Tommaso Occhipinti , Claudio Pernechele & Cesare Barbieri

To cite this article: Sergio Billotta , Massimiliano Belluso , Giovanni Bonanno , Salvatore di Mauro , Maria Cristina Timpanaro , Giovanni Condorelli , P. Giorgio Fallica , Massimo Mazzillo , Delfo Sanfilippo , Giuseppina Valvo , Luigi Cosentino , Paolo Finocchiaro , Alfio Pappalardo , Giampiero Naletto , Tommaso Occhipinti , Claudio Pernechele & Cesare Barbieri (2009) Characterization of detectors for the Italian Astronomical Quantum Photometer Project, Journal of Modern Optics, 56:2-3, 273-283, DOI: 10.1080/09500340802677068

To link to this article: https://doi.org/10.1080/09500340802677068

Journal of Modern Optics
Vol. 56, Nos. 2–3, 20 January–10 February 2009, 273–283

Taylor & Francis
Taylor & Francis Group

Characterization of detectors for the Italian Astronomical Quantum Photometer Project

Sergio Billotta[a]*, Massimiliano Belluso[a], Giovanni Bonanno[a], Salvatore di Mauro[a], Maria Cristina Timpanaro[a], Giovanni Condorelli[b], P. Giorgio Fallica[b], Massimo Mazzillo[b], Delfo Sanfilippo[b], Giuseppina Valvo[b], Luigi Cosentino[c], Paolo Finocchiaro[c], Alfio Pappalardo[c], Giampiero Naletto[d], Tommaso Occhipinti[d], Claudio Pernechele[e] and Cesare Barbieri[f]

[a]*INAF Astrophysical Observatory of Catania, Catania, Italy;* [b]*STMicroelectronics, Catania, Italy;* [c]*INFN – Laboratori Nazionali del Sud, Catania, Italy;* [d]*Department of Information Engineering, University of Padova, Padova, Italy;* [e]*INAF Astrophysical Observatory of Cagliari, Cagliari, Italy;* [f]*Department of Astronomy, University of Padova, Padova, Italy*

(*Received 16 June 2008; final version received 8 December 2008*)

In the framework of a national collaboration to bring Quantum Optics concepts to Astronomy, we are involved in finding suitable detectors for this novel application. At 'INAF Osservatorio Astrofisico di Catania' and 'INFN – Laboratori Nazionali del Sud' laboratories, measurements of electro-optical parameters, such as photon detection efficiency (PDE), linearity, dark counts and after pulsing probability, as well as of timing resolution, have been carried out. These measurements have been done on silicon detectors, such as single photon avalanche diode (SPAD) (both single element and array), and silicon photon multiplier (SiPM), operating in the photon counting regime.

Keywords: SPAD; SiPM; single photon detection; quantum astronomy; detectors characterization

1. Introduction

A few years ago a project to bring the time resolution of Astronomy well below the nanosecond regime [1] was started. The availability of suitable detectors capable of counting the arriving photons at the maximum speed possible becomes crucial for such projects and have led us to investigate the electro-optical characteristics of novel detectors. These activities began from the conceptual design of a focal plane instrument, named QuantEYE [2–4], for the OverWhelmingly Large Telescope (OWL) [5] of the European Southern Observatory. QuantEYE was conceived as the fastest photon counting astronomical photometer ever, with an array of 100 parallel channels, and capable of pushing the time tagging capabilities toward the 10ps region. A prototype of QuantEYE was built for the Asiago Observatory and takes the name AquEYE [3,6,7] Asiago Quantum Eye.

A detailed description of AquEYE is reported by Barbieri et al. [6] in this issue.

The activity carried out by our group, inside this organization, is the properties evaluation of two kinds of detectors:

- single photon avalanche diode (SPAD);
- silicon photon multiplier (SiPM);

both operating in the photon counting regime in continuous mode, and characterized by good quantum efficiency in the visible and ultra-fast response (tens to hundreds of picoseconds).

The SPAD [8,9] is a silicon sensor able to detect single photon events. It is essentially an avalanche photodiode that, biased above breakdown, remains quiescent until a carrier, generated either thermally or by a photon, triggers an avalanche. A quenching circuit (active or passive) extinguishes the avalanche and makes the pixel ready to detect another photon [9,10].

The SiPM [11], as the SPAD, is a photodetector operated in Geiger mode, with the difference that it is constituted by hundreds/thousands of pixels, and the discharge is quenched by a small polysilicon resistor (passive quenching) in each pixel. The independently operating pixels are connected to the same readout line; therefore the combined output signal corresponds to the sum of all fired pixels. It reaches an intrinsic gain for a single photoelectron of 10^6, comparable to that of vacuum phototubes (PMTs).

At INAF-OACt and INFN-LNS laboratories various measurements of timing resolution and of electro-optical characteristics, such as photon detection efficiency, linearity, dark and after pulsing, have been carried-out to select a suitable detector for QuantEYE. In this paper we present the experimental equipment used to characterize SPADs manufactured by MPD [12], SiPMs and SPADs array provided by

*Corresponding author. Email: sergio.billotta@oact.inaf.it

ISSN 0950–0340 print/ISSN 1362–3044 online

DOI: 10.1080/09500340802677068
http://www.informaworld.com

STMicroelectronics (STM) and multi-pixel photon counters (MPPCs) manufactured by Hamamatsu [13]. The measurements and some results are here also discussed and these clearly show that the MPD device is the one that at the moment can satisfy the project requirements (see [6]).

2. Experimental apparatus

The equipment used for the detector electro-optical characterization is one of the available facilities at 'INAF Osservatorio Astrofisico di Catania' laboratory. A detailed description of the experimental set up is reported in [14] and here the implemented main parts are briefly presented.

By following from right to left the scheme shown in the upper part of Figure 1 you can find: a Xenon lamp used as the radiation source, a wavelength selection system constituted essentially by a set of filters and a Czerny–Turner monochromator (FWHM better than 1 nm in the 130–1100 nm spectral range) a beam splitter to direct the monochromatic radiation towards an integrating sphere hosting a 1 cm^2 reference photodiode (NIST traced) and the detector to be characterized.

The photon flux intensity coming into the integrating sphere can be varied by means of several neutral filters or changing the aperture of the entrance or exit slits of the monochromator. Due to the very small size of the detectors to be characterized with respect to the optical beam we used an integrating sphere to spatially integrate the radiant flux and the reference photodiode measured the number of photons per unit area. Furthermore, we designed appropriate mechanical structures, in terms of aperture and distance from the centre of the sphere, to illuminate both detectors with the same radiant flux. The left side of Figure 2 shows the internal part of the mechanical structure hosting the photon counting detectors and where the active quenching circuit (AQC) takes place, while the right part shows the cold finger that supports the detector and allows one to operate the device at different temperatures down to $-30^{\circ}C$.

Apart from the MPD SPAD, the other SPAD detectors have been operated by an active quenching circuit (AQC) designed and realized at our laboratory. A schematic diagram of this circuit is shown in Figure 3. The SPAD is reverse biased through the cathode at $V_{break} + V_{ex}$, where V_{break} is a voltage a little lower than the breakdown and V_{ex} brings the total reverse bias over breakdown. When an avalanche is triggered, the current flowing on R_s activates the discriminator A, which varies the state of node 2, giving a pulse synchronized with the avalanche. A buffer provides for the output of the pulse. Two feedback loops are used, one to quench immediately the diode to reduce the charge trapping and then avoiding after-pulses, and the other to delay the system reset, keeping quenched the diode for a dead time T known as the hold-off time. The first feedback loop acts on S_1 switch forcing the diode anode at V_{ex} voltage, giving as the total voltage V_{break} and thus leaving the diode quenched. The hold-off time is user selectable. After the time T the discriminator B by means of the switch SL_1 forces the node 1 at ground voltage, making the SPAD ready for a new detection. At the same time the discriminators A and B open S_1 and switch SL_1 to V_{ex}.

The AQC output is connected to an Eagle Technology μ-DAQ USB-48c device counter. It acquires the counts from the AQC on the PC through a standard USB 2.0 connection. Simultaneously we measure the signal from the reference photodiode through the Keithley 6514 system electrometer that is connected through an IEEE 488 parallel interface to the PC. We realized an automated software procedure which controls the instruments, acquires the data in real time and calculates the PDE according to the different areas of the detectors. The minimum integration time of the system is 1 ms and the counter is 16 bit wide (65, 536 counts) that means the system safely measures up to about 10^7 counts per second (cnts s^{-1}).

The SPAD counting losses, due to the probability that a photon is absorbed in the pixel active area during the hold-off time, have been taken into account by using a conventional dead time correction method [15].

Each SPAD manufactured by MPD (Figure 4) is housed in a sealed module, the operating conditions are settled by the electronics inside the module, which includes also an AQC. The module has a TTL output, thus we directly connected the device output to the μ-DAQ counter.

For the SiPM characterization we used two Keithley ammeters: the Keithley 6514 system electrometer for SiPM and the Keithley 485 picoammeter for the reference photodiode. Both ammeters are controlled by a PC through a standard IEEE 488 interface.

All the measurements have been performed with a photon flux in the 10^8–10^{11} phs s^{-1} cm^{-2} range, which is sufficient to be detected by the reference photodiode and not too high to saturate the two types of photon counting detectors.

The time resolution measurements were carried out at INFN-LNS laboratories using a time-correlated single photon counting apparatus [15]. Figure 5 shows a schematic diagram of the apparatus, constituted essentially by a pulsed laser system ($\lambda = 408$ nm,

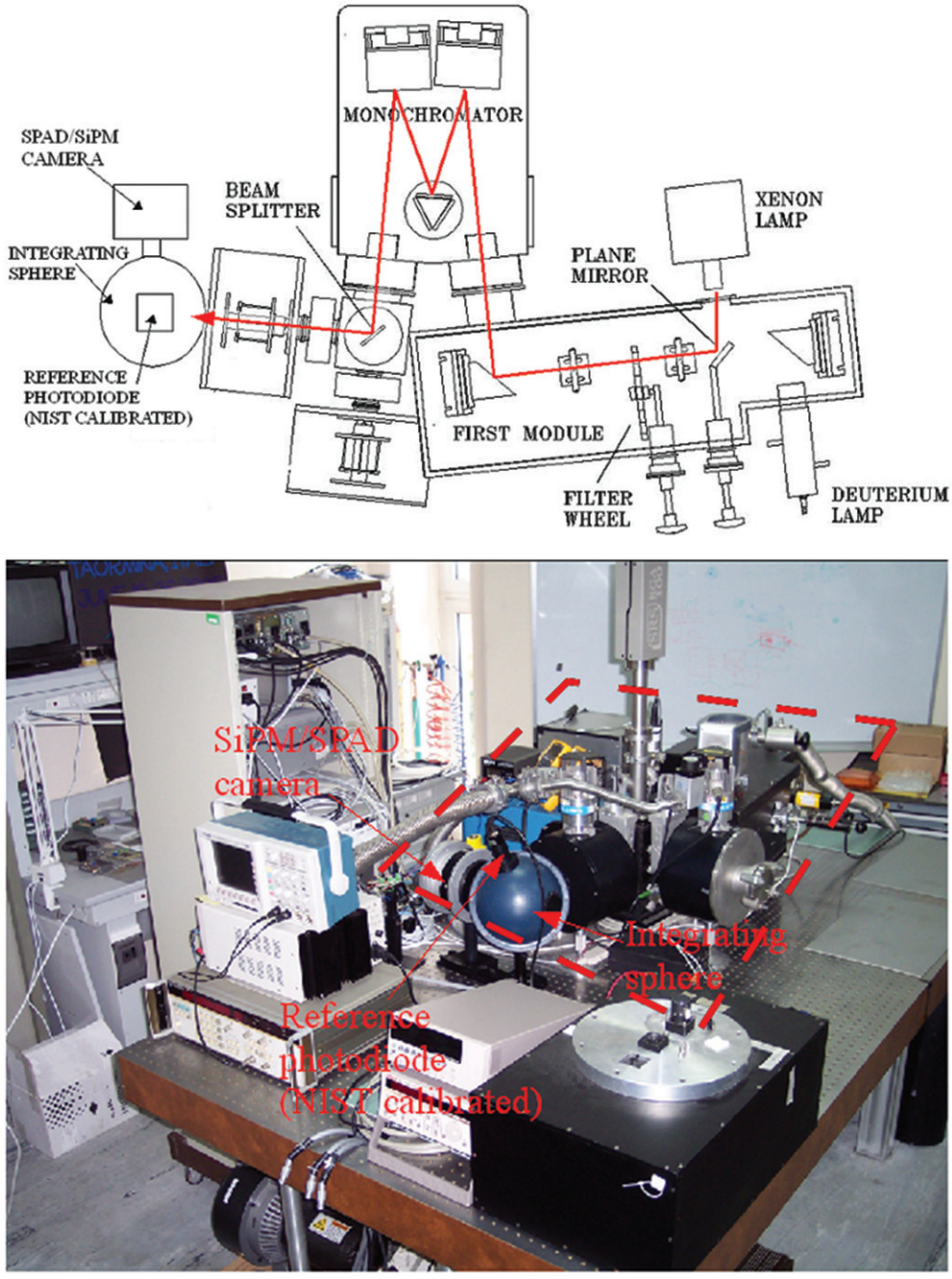

Figure 1. Top: scheme of the implemented mechanical and optical parts of the apparatus. The red line indicates the light path. A Xenon lamp is used as the radiation source, several filters and mirrors are used to obtain a bandwidth around the wavelength of interest and to focus the beam to the monochromator, which allows one to select a line in the 130–1100 nm spectral range with a FWHM better than 1 nm. The monochromatic light is directed by means of a beam splitter and focused through a lens inside an integrating sphere, in order to produce an uniform light. Bottom: image of the characterization apparatus developed at 'INAF Osservatorio Astrofisico di Catania', the dotted line delimits the implemented parts of the experimental set-up. (The colour version of this figure is included in the online version of the journal.)

$\sigma_t \approx 120$ ps), equipped with a multiple grey filter in order to reduce its intensity at will, and a time-to-amplitude converter (10 ps resolution) to build the distribution of the time intervals between the laser trigger and the photon detection on the SPAD.

3. First results

As mentioned above, several characterization campaigns have been carried-out at our laboratory on various SPADs [16] and SiPMs, manufactured by different companies.

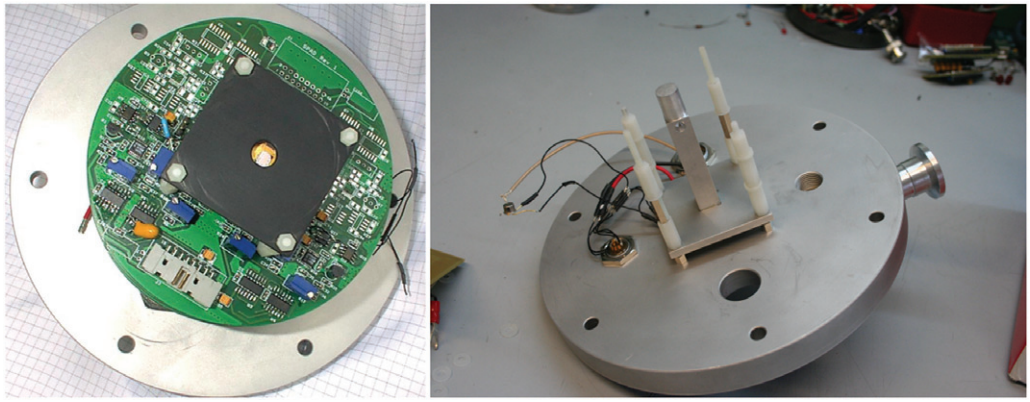

Figure 2. Internal part of the mechanical structure where the SPAD AQC electronics (left picture) and the cold finger (right picture), that hosts the detector and allows one to operate the device at different temperatures down to −30°C, are mounted. This camera has been realized to place the photon counting detectors at the same distance as the reference photodiode from the centre of the integrating sphere. (The colour version of this figure is included in the online version of the journal.)

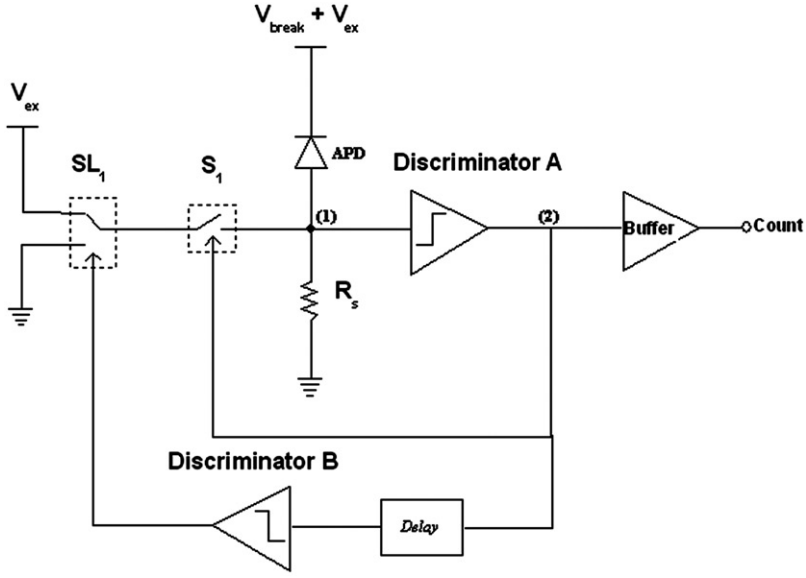

Figure 3. The SPAD is biased and driven by an active quenching circuit (AQC), designed and realized at the 'INAF – Osservatorio Astrofisico di Catania', that provides for extinguishing the avalanche, bringing the SPAD to its waiting conditions and after a changeable hold-off time making the SPAD ready to detect another photon, see text for more details. (The colour version of this figure is included in the online version of the journal.)

Table 1 lists the tested photon counting detectors with their relevant characteristics.

3.1. SPAD

In Figure 6 we report a plan view of a planar array fabricated by STMicroelectronics [17]. This is manufactured by the integration of 25 pixels with a square geometry of 5×5. STMicroelectronics has designed arrays with three different pixel diameters: 20, 40 and 60 μm. Separation distances between adjacent pixels are in the range of 160 and 240 μm according to different diameters. Anode contacts are in common for each row, while each cathode is separately contacted and available from outside by different pads. The typical breakdown voltage is about 30 V.

On these detectors we measured:

- dark counts;
- afterpulse;
- photon detection efficiency (PDE);
- time resolution.

We measured on various pixels of several SPAD arrays operating at room temperature and 20%

Figure 4. The MPD SPAD is housed in a sealed up module, the operating conditions, are settled by the electronics inside the module, which includes also an AQC. The module has a TTL output, NIM output, a TTL gating input to switch the detector off and a supply input connector. (The colour version of this figure is included in the online version of the journal.)

overvoltage dark count rates of about 4000 cnts s^{-1}, demonstrating a dark current which was quite uniform over all the sensitive area of each array. As an example, in Figure 7 the dark count rate at room temperature for a SPAD array with a 40 μm pixel diameter is shown. Apart from a pixel not working and one with too high dark current (due to high defectiveness), the SPAD array has an average dark count value of 3800 cnts s^{-1} (at 20% overvoltage) and a standard deviation of 20%.

In order to estimate the afterpulse [18] effects, we measured the dark count rate varying the hold off time by means of the AQC. The measurements have been carried out at different overvoltages. 80% of the tested devices show a modest presence of afterpulsing at low overvoltage and a moderate one at high overvoltage, as can be noted in Figure 8, which shows the dark count rate of a 50 μm pixel SPAD as a function of the hold off time for three different overvoltages.

The PDE was measured with the apparatus described in the previous paragraph. In general we found a peak at 600 nm that, depending on the bias voltage, has values from 40% to 60%. A PDE for a 40 μm device biased at 20% overvoltage is shown in Figure 9, a peak of about 60% at 600 nm is evident.

The timing was measured using a pulsed laser system mentioned in the previous paragraph; the measurements were performed in two different photon regimes: single-photon and multi-photon. The single-photon regime, achieved by strongly reducing the laser intensity, was verified by sending the photons onto a small piece of poly methyl methacrylate (PMMA) symmetrically coupled to two identical SPADs. We chose to operate in a regime where no coincidence between the two SPADs was observed (within 0.1%), thus implying that no two-photon events were detected in each SPAD. The resulting timing plot is reported in Figure 10, left, where we basically found a reconstruction of the laser pulse time structure reported in the operating manual, which confirms the validity of the method. We found $\sigma \approx 140$ ps that after a rough quadratic subtraction of the laser resolution points toward a ≈ 70 ps contribution from the SPAD and the electronics.

When increasing the intensity to the regime of several photons per event (≈ 5 to 20) by removing some of the filters, the probability of detecting one of the earliest photons is increased, thus improving the time resolution toward the intrinsic limit of the SPAD. Figure 10, right, shows the related histogram, with the expected $\sigma \approx 70$ ps that can be assumed as very close to the effective SPAD (plus electronics) resolution. The two distributions were fitted by means of a Gaussian with a right-hand exponential tail; the quoted sigma values are those for the Gaussian parts.

We also characterized one of the four MPD SPADs utilized for the AquEYE prototype.

The detector is a 50 μm SPAD and has a very good single photon timing resolution of 50 ps FWHM with the NIM timing output, a very low after pulse probability, lower than 1.5% (as reported by the manufacturer), and a dead time of 65 ns. As can be

noted from Figure 11 this device shows a PDE peak of about 60% at 550 nm and we have measured a dark count rate of 25 ± 15 cnts s^{-1}. All these features make the MPD device certainly good for the purpose of the scientific goal.

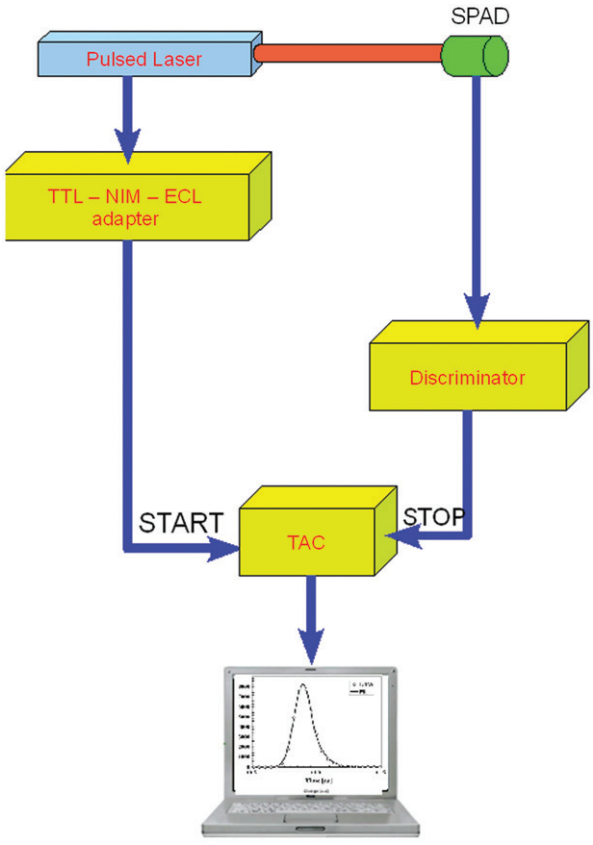

Figure 5. Scheme of the apparatus used at INFN-LNS laboratories for the time resolution measurements. A pulsed laser system equipped with a multiple grey filter illuminates a SPAD, at the same time the trigger from the laser sends the START to a time-to-amplitude converter (TAC). When the SPAD detects the photon from the laser it sends the STOP to the TAC. The TAC is connected to a PC to build the distribution of the time intervals between the laser trigger and the photon detection on the SPAD. (The colour version of this figure is included in the online version of the journal.)

3.2. SiPM

Another suitable detector for the quantum astronomy project is the SiPM device. In fact this device, besides the same SPAD time tagging characteristics, has the advantage of a larger area than that of the SPAD. A larger active area surely helps in optically coupling the detector to large telescope pupils and in reducing detector alignment difficulties. Furthermore, this kind of device can detect more photons simultaneously. However, not all the surface is able to detect photons, thus we have to take into account the fill factor to measure the PDE parameter.

We have characterized some new STM prototypes and an Hamamatsu multi pixel photon counter (MPPC).

We measured the PDE of a $1 \times 1\,mm^2$ STM SiPM with 400 pixels and a fill factor of 41%, applying an overvoltage of 4 V and setting the working temperature at 24°C. The resulting plot is shown in Figure 12, which indicates a peak of about 35% at 500 nm.

With the above-mentioned apparatus, illuminating the device with an increasing flux at 400 nm wavelength, we measured the current response from the SiPM, and a very good linearity response was derived over a range of 2×10^7–35×10^7 phs s^{-1} on the SiPM device (Figure 13).

As mentioned, we have also tested an Hamamatsu MPPC S10362-11-050C. This device, as the STM prototype, is a $1 \times 1\,mm^2$ with 400 pixels but with a fill factor of 61% and an operating voltage of 69.84 V. At room temperature (25°C) we found a PDE (Figure 14) that was in the range of 25%–30% between 350 and 550 nm, comparable to the STM SiPM.

Both devices have a PDE peak of about 30%, about half of the typical SPAD PDE, and this is essentially due to the small fill factor of a SiPM. Furthermore, this value is enhanced by the afterpulsing contribution, thus measurements to evaluate this noise are in progress in order to correct the SiPM PDE. Such characteristics make these detectors, at the moment, not good candidates for our scientific project. Future

Table 1. Tested photon counting detectors with the relevant characteristics.

Detector type	Manufacturer	Diameter of the sensitive area	Number of pixels	PDE	Dark	Time jitter
SPAD	STMicroelectronics	20 to 60 μm	Array of 25 pixels	40%–60% @ 600 nm	~4000 cnts s^{-1} @ room temperature	70 ps
SPAD	MPD	50 μm	single	60% @ 550 nm	25 cnts s^{-1} @ −20°C	50 ps
SiPM	STMicroelectronics	32 μm	400	35% @ 500 nm	1.8×10^{-6} A @ 24°C	Under testing
MPPC	Hamamatsu	50 μm	400	25%–30% @ 350–550 nm	7.6×10^{-8} A @ 25°C	Under testing

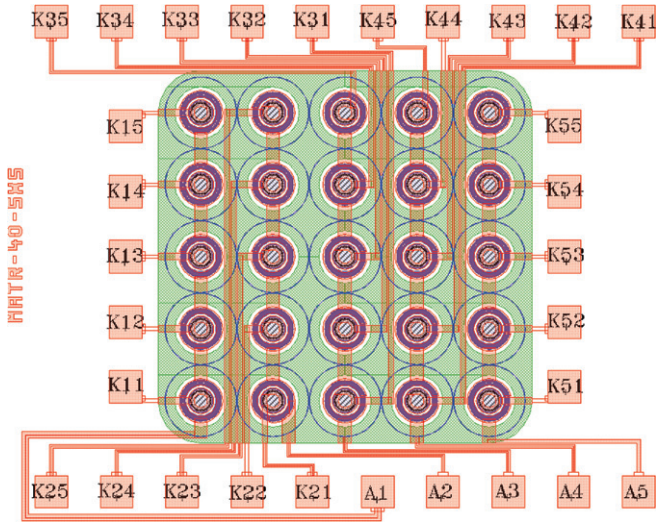

Figure 6. Plan view of an array fabricated by STMicroelectronics. This device is manufactured by the integration of 25 pixels with a square geometry of 5×5. (The colour version of this figure is included in the online version of the journal.)

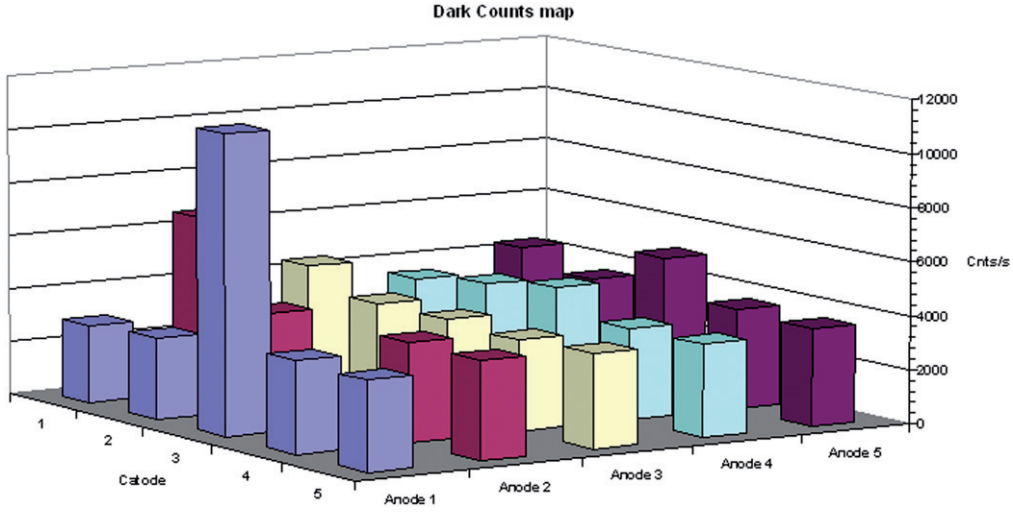

Figure 7. Dark count rate of a SPAD array of 40 µm diameter dimension for each pixel obtained at room temperature. The SPAD array has, apart from two pixels, respectively, with too high and too low dark count rate, a low average dark count value of 3680 cnts s^{-1} (at 20% overvoltage) and a standard deviation of 25%. (The colour version of this figure is included in the online version of the journal.)

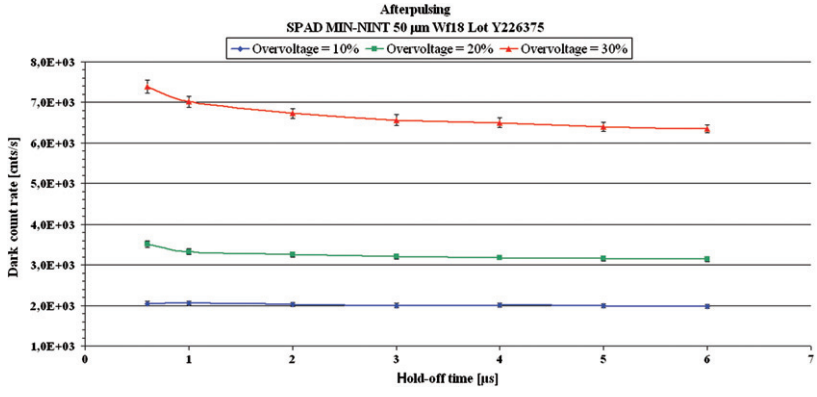

Figure 8. Dark count rate of a 50 µm pixel as a function of the hold off time for three different overvoltages. (The colour version of this figure is included in the online version of the journal.)

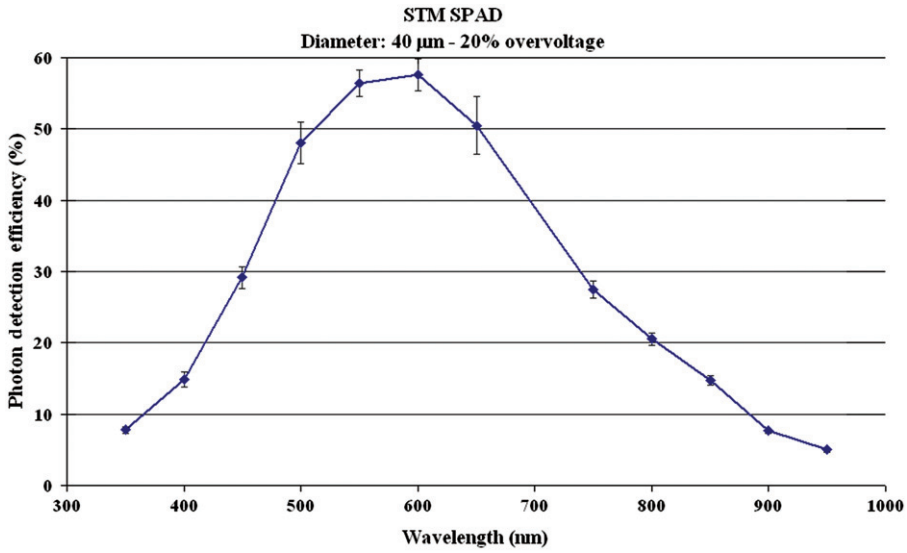

Figure 9. PDE for a STM 40 µm device biased at 20% overvoltage; we can note the peak of about 60% at 600 nm. (The colour version of this figure is included in the online version of the journal.)

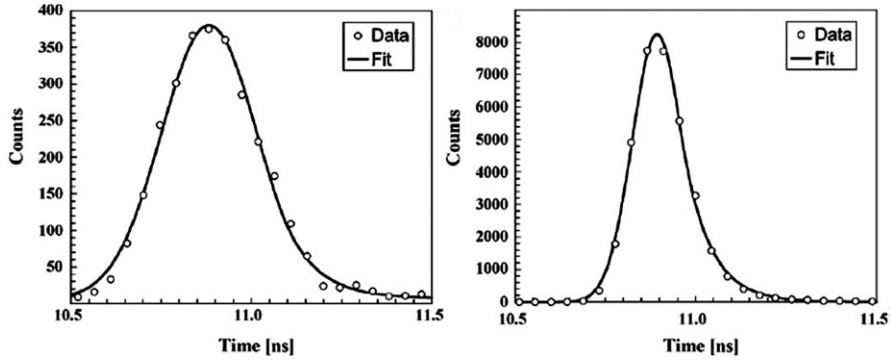

Figure 10. Time resolution measurements. We found that, as expected, when operating in the single photon regime (left figure) the measured timing reflects the time structure of the laser pulse; conversely, when operating in the multi-photon regime (right figure) the overall time resolution improves toward the intrinsic resolution of the SPAD, that is about $\sigma_t \approx 70$ ps (which also includes the electronics contribution). The rough quadratic subtraction of the 120 ps laser width from the measured 140 ps single photon width (left) yields the expected 70 ps of the multi-photon time spectrum (right). (The colour version of this figure is included in the online version of the journal.)

improvements are necessary: larger pixels to provide greater fill factor and better structure to lower the dark current. We are confident that SiPM devices in the near future can be considered a valid substitution for SPAD devices, especially for imaging applications.

4. Conclusions

Our investigation to select the best detectors for a quantum astronomy instrument has shown that, at present, the SPAD is the detector which better fits the project requirements. The MPD module used for our prototype has shown a good PDE (60% @ 550 nm), a very low dark count rate (25 cnts s^{-1}) and a fast response (better than 50 ps FWHM). The obvious disadvantage is the small sensor area, which forces one to have an additional relay optics and causes a great deal of attention to be paid to detector alignment.

The SiPM is a larger detector, and with some companies developing arrays up to 2.5 cm^2, its timing and signal response should be similar to the SPAD, but typically it has a lower PDE, due to the low fill factor, and a higher dark count rate. However, the SiPM is a very recent detector, and future technological

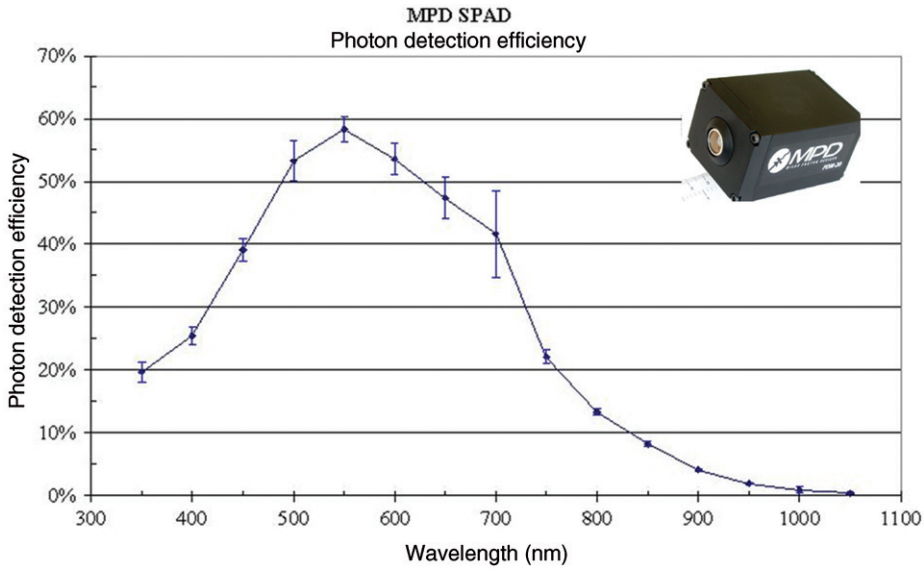

Figure 11. Photon detection efficiency of one of the four MPD SPADs utilized now for the AquEYE prototype. This device shows a PDE peak of about 60% at 550 nm. (The colour version of this figure is included in the online version of the journal.)

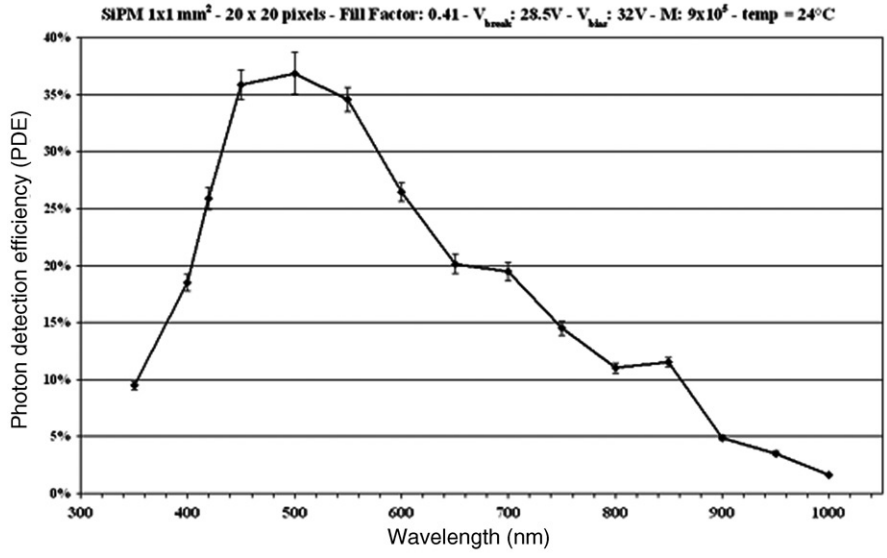

Figure 12. PDE of a $1 \times 1\,\text{mm}^2$ STM SiPM with 400 pixels and a fill factor of 41%, applying an overvoltage of 4 V and setting the working temperature at 24°C. A peak of about 35% at 500 nm is clearly evident. (The colour version of this figure is included in the online version of the journal.)

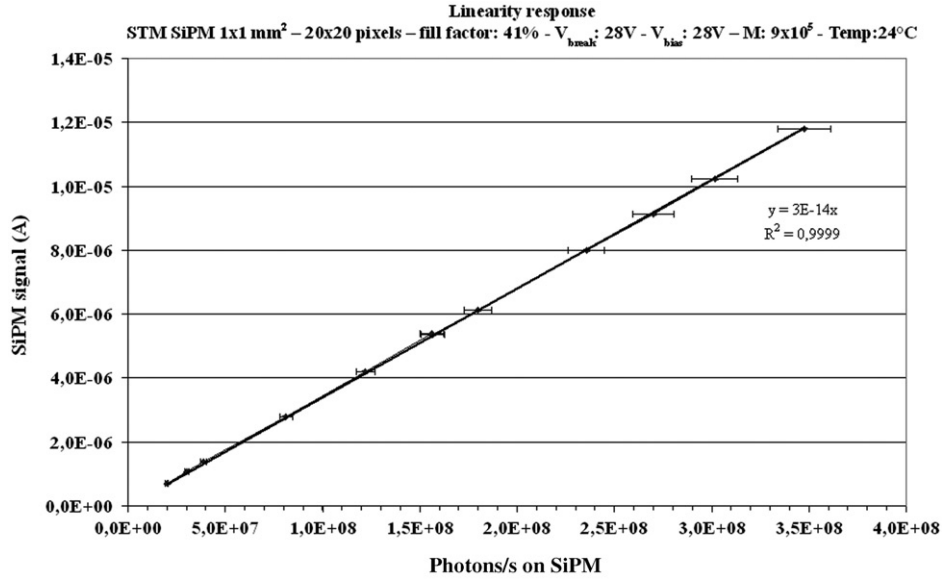

Figure 13. Linearity response of a $1 \times 1\,\text{mm}^2$ STM SiPM with 400 pixels and a fill factor of 41%, applying an overvoltage of 4 V and setting the working temperature at 24°C. We can note a very good linearity response up to 3.5×10^8 photons per second. (The colour version of this figure is included in the online version of the journal.)

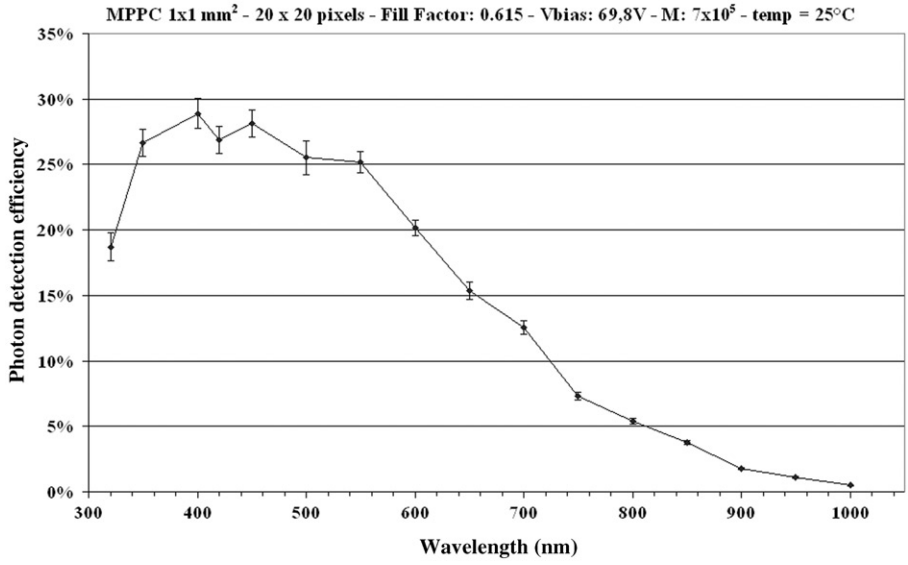

Figure 14. PDE of the Hamamatsu MPPC S10362-11-050C at room temperature. It is in the range of 25%–30% between 350 and 550 nm. (The colour version of this figure is included in the online version of the journal.)

progress could yield SiPMs that can efficiently replace the SPAD. In this framework we are collaborating with STMicroelectronics in the development of new SiPM devices.

Acknowledgements

Work was partly funded by the Ministry of University and Research and the National Institute for Astrophysics (INAF) through PRIN 2006.

References

[1] Barbieri, C.; Dravins, D.; Occhipinti, T.; Tamburini, F.; Naletto, G.; Da Deppo, V.; Fornasier, S.; D'Onofrio, M.; Fosbury, R.A.E.; Nilsson, R.; Uthas, H. *J. Mod. Opt.* **2007,** *54,* 191–197.

[2] Barbieri, C.; Da Deppo, V.; D'Onofrio, M.; Dravins, D.; Fornasier, S.; Fosbury, R.; Naletto, G.; Nilsson, R.; Occhipinti, T.; Tamburini, F.; Uthas, H.; Zampieri, L. QuantEYE, The Quantum Optics Instrument for OWL.. In *The Scientific Requirements for Extremely Large Telescopes*; Whitelock, P., Leibundgut, B., Dennefeld, M., Eds.; IAU Symposium Series 232, IAU: Cambridge University Press, 2006; pp 506–507.

[3] Naletto, G.; Barbieri, C.; Occhipinti, T.; Tamburini, F.; Billotta, S.; Cocuzza, S.; Dravins, D. Very Fast Photon Counting Photometers for Astronomical Applications: from QuantEYE to AquEYE. *SPIE Conference 6853A on Photon Counting Applications*; Prague, April 19, 2007.

[4] Naletto, G.; Barbieri, C.; Dravins, D.; Occhipinti, T.; Tamburini, F.; Da Deppo, V.; Fornasier, S.; D'Onofrio, M.; Fosbury, R.A.E.; Nilsson, R.; Uthas, H.; Zampieri, L. QuantEYE: A Quantum Optics Instrument for Extremely Large Telescopes. *Ground-Based and Airborne Instrumentation For Astronomy*, SPIE Proceedings 6269; 2006; DOI:10.1117/12.671184.

[5] OWL Concept Design Report; Technical report: ESO document OWL-TRE-ESO-0000-0001 Issue 2, 2005.

[6] Barbieri, C.; Naletto, G.; Occhipinti, T.; Facchinetti, C.; Verroi, E.; Giro, E.; Di Paola, A.; Billotta, S.; Zoccarato, P.; Bolli, P.; Tamburini, F.; Bonanno, G.; D'Onofrio, M.; Marchi, S.; Anzolin, G.; Capraro, I.; Messina, F.; Belluso, M.; Pernechele, C.; Zaccariotto, M.; Zampieri, L.; Da Deppo, V.; Fornasier, S.; Pedichini, F. *J. Mod. Opt.* **2009,** *56,* 261–272.

[7] Barbieri, C.; Billotta, S.; Bolli, P.; Bonanno, G.; Di Paola, A.; Facchinetti, C.; Giro, E.; Marchi, S.; Naletto, G.; Occhipinti, T.; Pernechele, C.; Sain, E.; Zaccariotto, M.; Zoccarato, P. *Status of AQUEYE, the Fast Multichannel Photometer for the 182 cm Telescope at Cima Ekar, Mem.* SAIt, Apr 17–20, 2007.

[8] Zappa, F.; Tisa, S.; Tosi, A.; Cova, S. *Sens. Actuators A* **2007,** *140,* 103–112.

[9] Cova, S.; Ghioni, M.; Lotito, A.; Rech, I.; Zappa, F. *J. Mod. Opt.* **2004,** *51,* 1267–1288.

[10] Cova, S.; Ghioni, M.; Lacaita, A.; Samori, C.; Zappa, F. *Appl. Opt.* **1996,** *35,* 1956–1976.

[11] Golovin, V.; Saveliev, V. *Nucl. Instrum. Meth. A* **2004,** *518,* 560–564.

[12] MPD. http://www.micro-photon-device.com (accessed Jan, 2008).

[13] Hamamatsu. http://sales.hamamatsu.com/assets/pdf/catsandguides/mppc_kapd0002e02.pdf (accessed Jan, 2008).

[14] Bonanno, G.; Bruno, P.; Cali, A.; Cosentino, R.; Di Benedetto, R.; Puleo, M.; Scuderi, S. Catania Astrophysical Observatory Facility for UV CCD Characterization. In *SPIE 2808, EUV, X-Ray, and Gamma-Ray Instrumentation for Astronomy VII*; Siegmund, O., Gummin, M., Eds.; SPIE Press: Bellingham, WA, 1996; pp 242–249.

[15] O'Connor, V.; Phillips, D. *Time-correleted Single Photon Counting;* Academic: London, 1984.

[16] Belluso, M.; Bonanno, G.; Billotta, S.; Calì, A.; Scuderi, S.; Mazzillo, M.; Fallica, P.G.; Sanfilippo, D.; Sciacca, E.; Lombardo, S. *Sci. Detectors Astron.* **2005,** *336,* 461–467.

[17] Mazzillo, M.; Condorelli, G.; Campisi, A.; Sciacca, E.; Belluso, M.; Billotta, S.; Sanfilippo, D.; Fallica, G.; Casentino, L.; Finocchiaro, P.; Musumeci, F.; Privitera, S.; Tudisco, S.; Lombardo, S.; Rimini, E.; Bonanno, G. *Sens. Actuators A* **2007,** *138,* 306–312.

[18] Giudice, A.C.; Ghioni, M.; Cova, S.; Zappa, F. *A Process and Deep Evaluation Tool: Afterpulsing in Avalanche Junctions*. In 33rd Conference on European Solid-State Device Research, Vol. 1; Estoril, Sept 16–18, 2003; IEEE: New York, pp 347–350.